

Experimental Time-Resolved Interference with Multiple Photons of Different Colors

Xu-Jie Wang,^{1,2,3} Bo Jing,^{1,2,3} Peng-Fei Sun,^{1,2,3} Chao-Wei Yang,^{1,2,3} Yong Yu,^{1,2,3} Vincenzo Tamma,^{4,5}
 Xiao-Hui Bao,^{1,2,3,*} and Jian-Wei Pan^{1,2,3,†}

¹*Hefei National Laboratory for Physical Sciences at Microscale and Department of Modern Physics,
 University of Science and Technology of China, Hefei, Anhui 230026, China*

²*CAS Center for Excellence and Synergetic Innovation Center in Quantum Information and Quantum Physics,
 University of Science and Technology of China, Hefei, Anhui 230026, China*

³*CAS-Alibaba Quantum Computing Laboratory, Shanghai 201315, China*

⁴*School of Mathematics and Physics, University of Portsmouth, Portsmouth PO1 3QL, United Kingdom*

⁵*Institute of Cosmology & Gravitation, University of Portsmouth, Portsmouth PO1 3FX, United Kingdom*



(Received 29 March 2018; revised manuscript received 26 June 2018; published 22 August 2018)

Interference of multiple photons via a linear-optical network has profound applications for quantum foundation, quantum metrology, and quantum computation. Particularly, a boson sampling experiment with a moderate number of photons becomes intractable even for the most powerful classical computers. Scaling up from small-scale experiments requires highly indistinguishable single photons, which may be prohibited for many physical systems. Here we report a time-resolved multiphoton interference experiment by using photons not overlapping in their frequency spectra from three atomic-ensemble quantum memories. Time-resolved measurement enables us to observe nonclassical multiphoton correlation landscapes, which agree well with theoretical calculations. Symmetries in the landscapes are identified to reflect symmetries of the optical network. Our experiment can be further extended to realize boson sampling with many photons and plenty of modes, which thus may provide a route towards quantum supremacy with nonidentical photons.

DOI: [10.1103/PhysRevLett.121.080501](https://doi.org/10.1103/PhysRevLett.121.080501)

Universal linear-optical quantum computing [1] is generally considered to be challenging in the near future. An intermediate quantum computing model, namely, “boson sampling” which requires less demanding experimental overheads [2], has attracted intensive experimental interest in recent years [3–11]. A boson sampling machine can be realized by interfering many single photons through a linear optical network. Sampling the output photon distribution is strongly believed to be intractable for a classical computer for large photon numbers [2,12]. For experimental realizations, photon indistinguishability is crucially important, since for distinguishable photons the computational complexity collapses to a polynomial scaling, which becomes tractable for a classical computer [12]. Requiring complete overlap in the photonic spectra as a way to achieve photon indistinguishability may impose a challenge for many types of photon sources, particularly the solid-state single photon emitters [13]. The inhomogeneous distribution of complex mesoscopic environment of the solid state tend to cause frequency distinguishability for photons created from different emitters.

Photon indistinguishability and interference are also very important fundamentally. The HOM dip is a beautiful manifestation of the interference of two identical photons [14–17]. When two photons are different in color, it was shown that high interference visibility can be recovered by

using time-resolved measurement [18,19]. Perfect coalescence can still happen when photons are detected simultaneously in the two output modes. Later it was studied that perfect entanglement swapping by interfering color-different photons is also possible by using time-resolved measurement and active feed forward [20]. Very recently, it has been shown that by using polarization- and time-resolved detections at the output of a random linear optical network, a much richer multiphoton correlation landscape can be observed for a boson sampling experiment with photons not overlapping in their temporal (frequency) spectra and/or with different polarizations [21,22]. Additionally, they showed that inner-mode correlation landscapes can manifest intriguing symmetric properties characterizing a given N -photon interferometer [22]. They also proved that boson sampling problems based on additionally sampling in the photonic inner modes and/or in the input photonic occupation numbers are at least as computationally hard as standard boson sampling [23–26].

In this Letter, we report a time-resolved three-photon interference experiment when no overlap occurs between the photonic spectra [21,22]. We make use of three cold atomic ensembles to create three independent single photons, which are injected into a linear optical network with its internal phase being adjustable. At the output ports of the network, the three photons are detected in a time-resolved

manner. We observe different kinds of multiphoton correlation landscapes as we change the phase configuration. The observed coincidence landscapes agree very well with theoretical calculations. Moreover, we also find that symmetries in the multiphoton coincidence landscape can reveal symmetries of the optical network [22]. Our work enables multiphoton interference to be recovered by using time-resolved measurements, and thus provides a route towards demonstrating quantum supremacy [26–28] with nonidentical photons.

In our experiment we make use of a versatile setup of cold atoms [29] to create single photons [30,31]. An atomic ensemble is captured and cooled through magneto-optical trapping (MOT). By employing the spontaneous Raman scattering process with a Λ energy scheme, we can create nonclassical correlations between a scattered photon and a spin wave excitation in a probabilistic way [32]. The spin wave excitation can be later retrieved as a second photon on demand. The experimental scheme is depicted in Fig. 1. To suppress high-order events, the excitation probability in the write process is typically very low. In order to enhance the photon generation rate, we make use of a dual Raman scattering process. A σ^+ polarized write-out photon heralds a $|2, -1\rangle_{F,mF}$ collective excitation. While a σ^- polarized write-out photon heralds a $|2, +1\rangle_{F,mF}$ collective excitation, and we conditionally apply a π pulse which transfers the $|2, +1\rangle_{F,mF}$ excitation to $|2, -1\rangle_{F,mF}$ excitation. The $|2, -1\rangle_{F,mF}$ excitation is later retrieved as a single photon on demand. Polarization multiplexing enables us to double the photon generation rate without increasing the contribution of high-order events.

To demonstrate multiphoton interference we make use of three similar setups to create three single photons as shown in Fig. 1. We first measure the single photon qualities. For each setup, we repeat the write process until a write-out photon is detected, and retrieve the heraldedly prepared spin wave excitation afterwards to a single photon. We measure the second-order autocorrelation $g^{(2)}$ in a standard procedure (see Ref. [33] and the Supplemental Material for details [34]) for the retrieved photon as a function of retrieval time. Within a storage duration of 50 μs , we find that the parameter $g^{(2)}$ hardly changes for each setup. We also change the excitation probability p_e and measure the parameter $g^{(2)}$ accordingly for each setup, with the results shown in Table I. Each value is averaged over the range of 0 ~ 50 μs . The $g^{(2)}$ parameter under the same write-out probability is nearly the same for three setups. In our experiment, we set the excitation probability to be $p_e = 0.04$ by making compromise between the single-photon generating rate and the single-photon quality.

It is crucial for a multiphoton interference experiments that many single photons are released simultaneously. For traditional photon sources like spontaneous parametric down-conversion or spontaneous four-wave mixing, this requirement imposes a scalability issue, since heralded

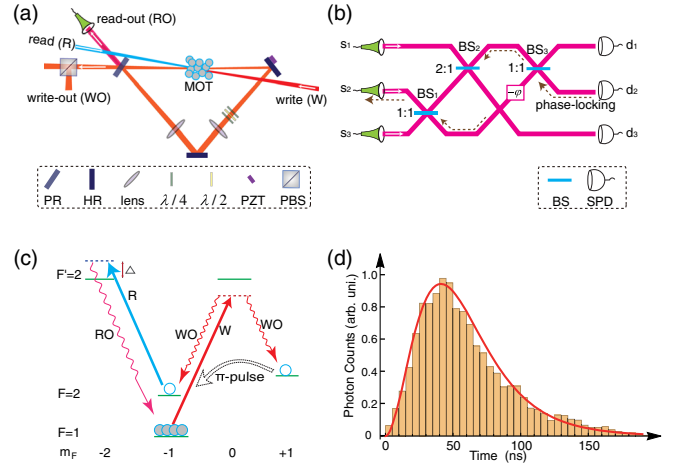


FIG. 1. Experimental setup. (a) Schematic diagram for one setup of atomic ensemble quantum memory to create one single photon. A ring cavity, which mainly consists of one partially reflecting mirror [(PR), $R \approx 80\%$] and two highly reflecting mirrors [(HR), $R \geq 99.9\%$], is used to enhance the single photon generation rate. The half- and quarter-wave plates ($\lambda/2$ and $\lambda/4$) in the cavity are used for polarization compensation. The cavity is intermittently locked by a piezoelectric ceramic transducer (PZT). In our multiphoton interference experiment, we make use of three similar setups to create three single photons. (b) Linear optic network for interference. The network is mainly composed of three beam splitters (BS, $R:T = 1:1$ or $2:1$). Single-mode fibers are used for the input and output modes. Heralding efficiency for a single photon at each input mode is 45%. (c) Atomic levels used in the single-photon source. Atoms are prepared at state $|1, -1\rangle_{F,mF}$ by optical pumping during each write process. After applying the write pulse, there are two orthogonal polarized write-out photons collected, once the spin wave is produced in state $|2, +1\rangle_{F,mF}$, a π pulse is applied to transfer the excitation to state $|2, -1\rangle_{F,mF}$. (d) A typical read-out single-photon profile. The histogram is a measured photon counts distribution by a single-photon detector during coincidence measurement. The solid line represent the read-out photon profile that we used in theoretical calculation. The full temporal width at half maximum for the wave packet is 63 ns.

photons are generated randomly in time and simultaneous creation is rare. An additional quantum memory may be employed to solve this issue [35,36]. In our experiment, however, the on-demand character of the photon source directly enables us to create multiple photons in an efficient way. If the memory lifetime is long enough, we can simply repeat the write process for setup until success and simultaneously retrieve three photons when all setups are

TABLE I. Measurement of $g^{(2)}$ for three setups.

p_e	0.01	0.02	0.03	0.04	0.06
$g^{(2)}(s_1)$	0.072(7)	0.126(9)	0.201(11)	0.233(11)	0.322(12)
$g^{(2)}(s_2)$	0.094(9)	0.165(10)	0.222(11)	0.279(11)	0.335(13)
$g^{(2)}(s_3)$	0.110(9)	0.142(8)	0.220(10)	0.251(10)	0.361(13)

ready. While our current setup has a limited lifetime ($\sim 64 \mu\text{s}$), thus we set a maximal trial number of $m = 7$. If less than three setups are ready when maximal trial limit is met, we restart the preparation process, otherwise we retrieve the three photons simultaneously. Such a preparation process enhances the n photon rate by a factor of $[1 - (1 - p_e)^m]/(mp_e^n)$.

The prepared multiple single photons are coupled into a multiphoton interferometer, which is constructed using bulk linear optics as shown in Fig. 1(b). The internal phase is actively stabilized to an adjustable value φ . Photons at each output mode are detected with a single-photon detector (SPD). All detected events are registered with a multichannel time-to-digit converter (TDC), and from which we can analyze multifold temporal correlations. The time resolutions of SPD and TDC are 350 and 50 ps, respectively. To demonstrate multiphoton interference with color-different photons, we set the three photons to be blue detuned by $2\pi \times 72.4$ (s_1), $2\pi \times 33.0$ (s_2), $2\pi \times 52.4$ MHz (s_3) relative to the $D1$ -line transition $|F = 1\rangle \leftrightarrow |F' = 2\rangle$ by adjusting the read beam frequency accordingly for each source. We make measurements for a number of different phases φ , and analyze multiphoton temporal correlations, with results shown in Figs. 2(a)–2(d).

We find that the correlation landscapes have very interesting structures, and changes remarkably as we change the phase φ associated with the ideal unitary transformation (reconstructed ones given in Supplemental Material [34])

$$U(\varphi) = \frac{1}{\sqrt{3}} \begin{bmatrix} -1 & (\sqrt{3}e^{-i\varphi} - 1)/2 & i(\sqrt{3}e^{-i\varphi} + 1)/2 \\ i & i(\sqrt{3}e^{-i\varphi} + 1)/2 & (1 - \sqrt{3}e^{-i\varphi})/2 \\ 1 & -1 & i \end{bmatrix}.$$

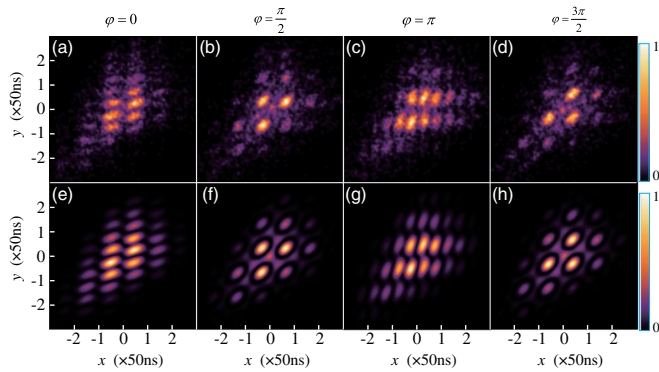


FIG. 2. Temporal correlation landscapes under different phase configurations. Plots in the first row are experimental results (a)–(d). The horizontal axis x in each plot refers to $(t_1 - t_3)$, while the vertical axis y refers to $(t_2 - t_3)$. Each point corresponds to a collection of events centered around (x, y) with a weighting function in the form of $e^{-[(x-x_i)^2 + (y-y_i)^2]/r_0^2}$, where (x_i, y_i) refers to the coordinate of a nearby threefold event and the parameter r_0 is chosen to be 3 ns to compromise between the fluctuation of event counts and reduction of pattern resolution. Plots in the second row are theoretical results (e)–(h).

In the case of $\varphi = 0$ the permanent of U is 0, which means that interference occurs destructively for all multiphoton paths if the input photons are perfectly identical each other. Thus, no threefold coincidence will be detected at the output modes. In our experiment, however, the input photons have different frequencies ($\Delta\omega \geq \delta\omega$, $\delta\omega = 2\pi \times 12.9$ MHz is the transform-limited linewidth). Nevertheless, the adoption of fast detection enables us to erase the color information, and destructive interference can be recovered if the three photons are detected simultaneously [21]. This is clearly proved by Fig. 2(a), as the region around (0,0) is rather dim in comparison with the peaks nearby. Departing from the dip, we observe beating patterns both in the direction of $x \equiv t_1 - t_3$ and $y \equiv t_2 - t_3$ [21]. Based on our Fourier analysis, beating in the x direction has a period of 51.4(11) ns, which is mainly due to interference of photon s_1 and photon s_3 . While beating in the y direction has a period of 24.9(3) ns, which is mainly due to interference of photon s_1 and photon s_2 . In the case of $\varphi = \pi/2$, the interferometer acts effectively as a symmetric tritter which is described as $U_{ds} = e^{-i2\pi ds/3}/\sqrt{3}$, where $s = 1, 2, 3$ refers to the modes at the source side and $d = 1, 2, 3$ refers to the modes at the detector side. The multiphoton correlation landscape has a quite different structure, as shown in Fig. 2(b) [22]. At the center point, it corresponds to the case of identical photons, for which the output of this tritter is either one photon in each mode or three photons in a same mode [37]. Away from the center point, the interference period is measured to be 49.7(7) and 50.3(13) ns, respectively, for the direction x and y , which are mainly due to equal contribution of all three pairwise interferences of the three input photons [22].

We also find that the observed correlation landscapes have some symmetries which may reflect symmetries either of the photons or the linear optic network [22]. When φ is switched from 0 to π or from $\pi/2$ to $3\pi/2$, it is the equivalent of interchanging the mode label 1 and 2 after BS_3 . Therefore, the correlation landscape of $\varphi = \pi$ ($3\pi/2$) should look the same as the landscape of $\varphi = 0$ ($\pi/2$) if we interchange the axis x and y . This is clearly proved by our result shown in Figs. 2(c) and 2(d), comparing with Figs. 2(a) and 2(b), respectively. Moreover, in the case of $\varphi = \pi/2$ or $3\pi/2$ the network acts as a symmetric tritter, which should give rise to a threefold symmetry in the correlation landscapes [22]. Therefore, we replot our experimental data in a three-dimensional coordinate as shown in Fig. 3. Each data point represents a threefold coincidence event at the time coordinate (t_1, t_2, t_3) . We can clearly identify a threefold rotational symmetry around the axis (1,1,1).

To further evaluate our experimental results, we also calculate the theoretical landscapes and make comparisons. By modeling the temporal wave packet with a function shown in Fig. 1(d), and using the reconstructed transfer matrices, we get the theoretical landscapes as shown in Figs. 2(e)–2(h). Apparently the experimental and theoretical

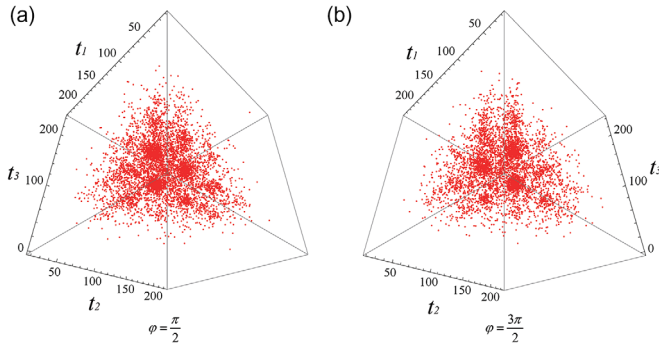


FIG. 3. Measured temporal correlation landscapes in a three-dimensional coordinate. (a) φ is set to $\pi/2$. (b) φ is set to $3\pi/2$. Both plots are viewed along the direction (1,1,1). Each data point represents a three-photon coincidence event registered at (t_1, t_2, t_3) .

landscapes resemble each other very well. To make a quantitative evaluation, we define a fidelity function as [5]

$$F = \frac{\sum_{i,j}^{N,M} f_e(x_i, y_j)^{1/2} f_t(x_i, y_j)^{1/2}}{[\sum_{i,j}^{N,M} f_e(x_i, y_j)]^{1/2} [\sum_{i,j}^{N,M} f_t(x_i, y_j)]^{1/2}},$$

where $f_e(x, y)$ is the experimentally measured probability distribution function, and $f_t(x, y)$ is the theoretical distribution. F gets its maximal value of 1 for two of the same landscapes. Calculated fidelities for different phases are $F(0) = 0.946$, $F(\pi/2) = 0.930$, $F(\pi) = 0.953$, $F(3\pi/2) = 0.925$, respectively, and give an average value of $\bar{F} = 0.939(13)$. According to our estimation (see Supplemental Material [34] for details), the limited $g^{(2)}$ values make a major contribution to the infidelity, and set a ceiling value of $F = 0.976$. We attribute the remaining gap due to inhomogeneity of pulse shape, phase stability of the linear optic network, and frequency drift of the single photons, etc.

In summary, we have demonstrated a time-resolved multiphoton interference with color-different photons. The observed correlation landscapes have very rich structures and shows some form of symmetry which is inherently related to symmetries of the linear-optic network. Besides, the adoption of memory-based photon sources enables efficient creation of the multiphoton state via feedback. Moreover, the method of using color-different photons mitigates the requirement in generating identical photons significantly for many physical systems. By employing a deterministic approach of photon creation and efficient coupling, scalably extending the current experiment to interfere more disparate photons through a much more complicated network will become possible in the near future, and may lead to quantum supremacy with photons in a conceptually new way [23,24]. This work also motivates future demonstration of the computational hardness of boson sampling with input photons of random colors and/or random occupation numbers [26],

as well as novel schemes for the characterization of the evolution of arbitrary single photon states in linear optical networks [21,22,38].

This work was supported by the National Key R&D Program of China (No. 2017YFA0303902), Anhui Initiative in Quantum Information Technologies, National Natural Science Foundation of China, and the Chinese Academy of Sciences. V. T. acknowledges partial support from the Army Research Laboratory under Cooperative Agreement No. W911NF-17-2-0179. V. T. also acknowledges useful discussions with Simon Laibacher.

X.-J. W. and B. J. contributed equally to this work.

*xhbao@ustc.edu.cn

†pan@ustc.edu.cn

- [1] P. Kok, W. J. Munro, K. Nemoto, T. C. Ralph, J. P. Dowling, and G. J. Milburn, *Rev. Mod. Phys.* **79**, 135 (2007).
- [2] S. Aaronson and A. Arkhipov, in *Proceedings of the Forty-Third Annual ACM Symposium on Theory of Computing* (ACM, New York, NY, USA, 2011), p. 333.
- [3] J. B. Spring, B. J. Metcalf, P. C. Humphreys, W. S. Kolthammer, X.-M. Jin, M. Barbieri, A. Datta, N. Thomas-Peter, N. K. Langford, D. Kundys, J. C. Gates, B. J. Smith, P. G. R. Smith, and I. A. Walmsley, *Science* **339**, 798 (2013).
- [4] M. A. Broome, A. Fedrizzi, S. Rahimi-Keshari, J. Dove, S. Aaronson, T. C. Ralph, and A. G. White, *Science* **339**, 794 (2013).
- [5] M. Tillmann, B. Dakić, R. Heilmann, S. Nolte, A. Szameit, and P. Walther, *Nat. Photonics* **7**, 540 (2013).
- [6] A. Crespi, R. Osellame, R. Ramponi, D. J. Brod, E. F. Galvão, N. Spagnolo, C. Vitelli, E. Maiorino, P. Mataloni, and F. Sciarrino, *Nat. Photonics* **7**, 545 (2013).
- [7] N. Spagnolo, C. Vitelli, M. Bentivegna, D. J. Brod, A. Crespi, F. Flamini, S. Giacomini, G. Milani, R. Ramponi, P. Mataloni, R. Osellame, E. F. Galvão, and F. Sciarrino, *Nat. Photonics* **8**, 615 (2014).
- [8] J. Carolan, J. D. a. Meinecke, P. J. Shadbolt, N. J. Russell, N. Ismail, K. Wörhoff, T. Rudolph, M. G. Thompson, J. L. O'Brien, J. C. F. Matthews, and A. Laing, *Nat. Photonics* **8**, 621 (2014).
- [9] J. Carolan, C. Harrold, C. Sparrow, E. Martin-Lopez, N. J. Russell, J. W. Silverstone, P. J. Shadbolt, N. Matsuda, M. Oguma, M. Itoh, G. D. Marshall, M. G. Thompson, J. C. F. Matthews, T. Hashimoto, J. L. O'Brien, and A. Laing, *Science* **349**, 711 (2015).
- [10] M. Bentivegna, N. Spagnolo, C. Vitelli, F. Flamini, N. Viggianiello, L. Latmiral, P. Mataloni, D. J. Brod, E. F. Galvao, A. Crespi, R. Ramponi, R. Osellame, and F. Sciarrino, *Sci. Adv.* **1**, e1400255 (2015).
- [11] H. Wang, Y. He, Y.-H. Li, Z.-E. Su, B. Li, H.-L. Huang, X. Ding, M.-C. Chen, C. Liu, J. Qin *et al.*, *Nat. Photonics* **11**, 361 (2017).
- [12] P. P. Rohde and T. C. Ralph, *Phys. Rev. A* **85**, 022332 (2012).

- [13] I. Aharonovich, D. Englund, and M. Toth, *Nat. Photonics* **10**, 631 (2016).
- [14] C. O. Alley and Y. H. Shih, in *Proceedings of the Second International Symposium on Foundations of Quantum Mechanics in the Light of New Technology* (Physical Society of Japan, Tokyo, 1986), p. 47.
- [15] C. K. Hong, Z. Y. Ou, and L. Mandel, *Phys. Rev. Lett.* **59**, 2044 (1987).
- [16] Y. H. Shih and C. O. Alley, *Phys. Rev. Lett.* **61**, 2921 (1988).
- [17] I. Walmsley, *Science* **358**, 1001 (2017).
- [18] T. Legero, T. Wilk, A. Kuhn, and G. Rempe, *Appl. Phys. B* **77**, 797 (2003).
- [19] T. Legero, T. Wilk, M. Hennrich, G. Rempe, and A. Kuhn, *Phys. Rev. Lett.* **93**, 070503 (2004).
- [20] T.-M. Zhao, H. Zhang, J. Yang, Z.-R. Sang, X. Jiang, X.-H. Bao, and J.-W. Pan, *Phys. Rev. Lett.* **112**, 103602 (2014).
- [21] V. Tamma and S. Laibacher, *Phys. Rev. Lett.* **114**, 243601 (2015).
- [22] S. Laibacher and V. Tamma, [arXiv:1706.05578](https://arxiv.org/abs/1706.05578) [*Phys. Rev. A* (to be published)].
- [23] S. Laibacher and V. Tamma, *Phys. Rev. Lett.* **115**, 243605 (2015).
- [24] V. Tamma and S. Laibacher, *Quantum Inf. Process.* **15**, 1241 (2016).
- [25] V. Tamma, *Int. J. Quantum. Inform.* **12**, 1560017 (2014).
- [26] S. Laibacher and V. Tamma, [arXiv:1801.03832](https://arxiv.org/abs/1801.03832).
- [27] J. Preskill, [arXiv:1203.5813](https://arxiv.org/abs/1203.5813).
- [28] A. W. Harrow and A. Montanaro, *Nature (London)* **549**, 203 (2017).
- [29] S.-J. Yang, X.-J. Wang, X.-H. Bao, and J.-W. Pan, *Nat. Photonics* **10**, 381 (2016).
- [30] S. Chen, Y.-A. Chen, T. Strassel, Z.-S. Yuan, B. Zhao, J. Schmiedmayer, and J.-W. Pan, *Phys. Rev. Lett.* **97**, 173004 (2006).
- [31] D. N. Matsukevich, T. Chanelière, S. D. Jenkins, S.-Y. Lan, T. A. B. Kennedy, and A. Kuzmich, *Phys. Rev. Lett.* **97**, 013601 (2006).
- [32] L. M. Duan, M. D. Lukin, J. I. Cirac, and P. Zoller, *Nature (London)* **414**, 413 (2001).
- [33] P. Grangier, G. Roger, and A. Aspect, *Europhys. Lett.* **1**, 173 (1986).
- [34] See Supplemental Material at <http://link.aps.org/supplemental/10.1103/PhysRevLett.121.080501> for more experimental details.
- [35] F. Kaneda, B. G. Christensen, J. J. Wong, H. S. Park, K. T. McCusker, and P. G. Kwiat, *Optica* **2**, 1010 (2015).
- [36] F. Kaneda, F. Xu, J. Chapman, and P. G. Kwiat, *Optica* **4**, 1034 (2017).
- [37] N. Spagnolo, C. Vitelli, L. Aparo, P. Mataloni, F. Sciarrino, A. Crespi, R. Ramponi, and R. Osellame, *Nat. Commun.* **4**, 1606 (2013).
- [38] O. Zimmermann and V. Tamma, *Int. J. Quantum. Inform.* **15**, 1740020 (2017).